*Clays and Clay Minerals*, Vol. 52, No. 1, 1–13, 2004.

# ALTERATION OF KAOLINITE TO CANCRINITE AND SODALITE BY SIMULATED HANFORD TANK WASTE AND ITS IMPACT ON CESIUM RETENTION

HONGTING ZHAO, YOUJUN DENG, JAMES B. HARSH, MARKUS FLURY* AND JEFFREY S. BOYLE

Department of Crop and Soil Sciences, Center for Multiphase Environmental Research, Washington State University, Pullman, WA 99164, USA

**Abstract**—Caustic nuclear wastes have leaked from tanks at the US Department of Energy's Hanford site in Washington State (USA) causing hundreds of thousands of gallons of waste fluids to migrate into the underlying sediments. In this study, four simulant tank waste (STW) solutions, which are high in NaOH (1.4 and 2.8 mol/kg), $NaNO_3$ (3.7 mol/kg) and $NaAlO_2$ (0.125 and 0.25 mol/kg), were prepared and reacted with reference kaolinite KGa-1 and KGa-2 at 50 and 80ºC for up to 2 months. The structure and morphology of the resulting products were characterized using X-ray diffraction, scanning electron microscopy, and Fourier transform infrared spectroscopy. The products were also examined for cation exchange and $Cs^+$ sorption as a function of ionic strength and types of cations in the background solutions. Cancrinite and sodalite were the only new minerals observed in all of the conditions tested in this experiment. Two major chemical processes were involved in the reactions: dissolution of kaolinite and precipitation of cancrinite and sodalite. Increasing NaOH concentration and temperature, and decreasing $NaAlO_2$ concentration increased the transformation rate. Both cancrinite and sodalite appeared stable thermodynamically under the experimental conditions. The newly formed feldspathoids were vulnerable to acid attack and pronounced dissolution occurred at pH below 5.5. Cancrinite and sodalite can incorporate $NaNO_3$ ion pairs in their cages or channels. Sodium in cancrinite and sodalite was readily exchangeable by $K^+$, but less easily by $Cs^+$ or $Ca^{2+}$. The feldspathoid products sorb nearly an order of magnitude more $Cs^+$ than the unaltered kaolinite. The Cs adsorption is reduced by competing cations in the background solutions. At low ionic strength (0.01 M $NaNO_3$ or 0.005 M $Ca(NO_3)_2$), $Ca^{2+}$ was more competitive than $Na^+$. When the concentration of the background solution was increased 10 times, $Na^+$ was more competitive than $Ca^{2+}$.

**Key Words**—Cancrinite, Cation Exchange, Cesium Sorption, Feldspathoid, Hanford Waste Tanks, Kaolinite, Mineral Stability, Mineral Transformation, Sodalite.

## INTRODUCTION

Many single-shell tanks of the 177 nuclear waste tanks located at the US Department of Energy's Hanford Reservation near Richland, WA (USA) have leaked, allowing 0.6–1.4 million gallons of high-level nuclear waste fluids to migrate into the underlying coarse-textured, relatively unweathered sediments (Hanlon, 1996; Gephart and Lundgren, 1998). Tank sludge, arising from the Pu production and extraction procedures at the Hanford site, is chemically very complex and of extreme chemical conditions. In most cases, tank sludge has very high $NaNO_3$ (up to ~8 M), NaOH (pH >13), and aluminate concentrations (>0.1 M) (Serne *et al.*, 1998). The temperature in several tanks rose to >100ºC during storage and was reported as high as 160ºC in one tank (Pruess *et al.*, 2002). The temperature in the immediate neighborhood sediments was estimated as high as 120ºC, and in the sediments 20 m below the tanks could be as high as 70ºC (Pruess *et al.*, 2002).

Reaction of the leaked waste solution with the underlying soil and sedimentary matrix will potentially result in dissolution of native minerals and subsequent formation of new secondary mineral phases. These chemical reactions can alter mineral surface properties, as well as the porosity and flow paths of the surrounding porous media. The physicochemical and mineralogical alterations of the sediment matrix could together lead to significant changes in the fate and transport of tank contaminants. Recent studies have shown that cancrinite, a feldspathoid, was formed after reacting Hanford sediments or quartz with tank simulant solutions at 60–90ºC (Nyman *et al.*, 2000; Bickmore *et al.*, 2001). We have found another feldspathoid, sodalite, in addition to cancrinite, which formed upon reacting the Hanford sediments with tank simulant for five weeks at 68ºC (our unpublished data). To the best of our knowledge, the retention properties of these materials for radionuclides have not yet been addressed. Quartz, feldspar, hornblende, mica, chlorite, illite, kaolinite, smectite and calcite are the most common minerals in Hanford sediments (Serne *et al.*, 1998). We found that these minerals have different reactivities toward the simulant solutions (our unpublished data). Even though kaolinite is not the most abundant clay mineral in Hanford sediments, here we report kaolinite alteration results because this mineral had shown the fastest alteration rate and the final precipitates are common products in the reactions with Hanford sediments.

* E-mail address of corresponding author:
flury@mail.wsu.edu
DOI: 10.1346/CCMN.2004.0520101

Kaolinite reactions give a high yield of the new mineral phases and the simplest mineral composition to study the retention behavior of radioactive nuclides on the new minerals.

It is known that kaolinite is not stable under highly alkaline conditions and various zeolite and feldspathoids can form (Breck, 1974). For instance, at high molarity of KOH (0.1 to 4.0 M) and temperatures of 35 and 80ºC, kaolinite transformed, in sequence, to illite, KI-zeolite, phillipsite, and finally, K-feldspar (Bauer *et al.*, 1998). Kaolinite has been used as the Al and Si sources for zeolite synthesis. Linde Type A, X and Y zeolites, cancrinite, sodalite, faujasite, and several other types of zeolites have been synthesized from kaolinite (Dudzik and Kowalak, 1974; Buhl, 1991; Alberti *et al.*, 1994; Gualtieri *et al.*, 1997). For zeolite synthesis, most of the experiments were carried out at high temperatures (*e.g.* 220ºC) and high pressures in autoclaves. These conditions are not likely to occur in the sediments underlying the tanks at the Hanford site. In addition, the presence of high concentrations of electrolytes such as $NaNO_3$ in the leaked waste solution may alter the reaction path.

The objectives of this study were to study: (1) the mineral alteration of kaolinite after contacting simulant Hanford tank solutions; (2) the stability and ion-exchange properties of resulting precipitates; and (3) the sorption behavior of Cs, a common radioactive element of Hanford nuclear wastes, on the newly formed precipitates. We hypothesized that kaolinite, with a low $Cs^+$ sorption capacity, would be transformed to feldspathoids under conditions designed to mimic those under leaking high-level waste tanks. Such a transformation should enhance the sorption of $Cs^+$.

## MATERIAL AND METHODS

### *Kaolinite samples and their reaction with simulant solutions*

Two kaolinite samples, a highly crystalline KGa-1 kaolinite and a poorly crystalline KGa-2 kaolinite, were used as received from the Clay Minerals Society (CMS) Source Clay Repository (Columbia, Missouri). Four simulant tank waste solutions (STWs) were prepared. The concentration of each component was within the range reported in Hanford waste process fluids (Serne *et al.*, 1998). Sodium hydroxide, sodium aluminate and sodium nitrate were divided into portions and added incrementally to make the four solutions (Table 1). 10 g of KGa-1 or KGa-2 powder were mixed with STWs at a solid/solution ratio of 1/10 (w/v) in 250 mL Nalgene polypropylene centrifuge tubes. The tubes were capped and stored in an 80ºC oven for various time periods (1, 2, 4 and 8 weeks). The tubes were shaken for 5 min each day on a reciprocal shaker. One set of parallel reactions between KGa-1 and STWs was performed at 50ºC for 2 months. After incubation for the designed time, the solids in the tubes were separated by centrifugation and dialyzed with 12,000–14,000 Dalton MWCO dialysis tubing against deionized water until the electrical conductivity was <10 µS/cm. The untreated KGa-1 kaolinite was dialyzed for the Cs adsorption experiment. The samples were dried at 40ºC and ground gently to break apart aggregates. The samples reacted at 80ºC were coded according to kaolinite sources, simulant solutions and reaction time. For example, code 'KGa-1-STW1-4-weeks' denotes the resulting solid sample of KGa-1 reacted with STW1 for 4 weeks at 80ºC. The sodium aluminate used in this experiment was of technical grade supplied by Strem Chemicals (Newburyport, Massachusetts, USA). Other chemicals used were of analytical grade obtained from Fisher Scientific or Aldrich.

### *Characterization of new mineral phases*

X-ray diffraction (XRD) analyses were performed on a Philips diffractometer with CuKα radiation (Philips XRG 3100, Philips Analytical Inc., Mahwah, New Jersey, USA) operated at 35 kV and 30 mA. Step-scan mode was used during the XRD analysis with a step size of 0.05º2θ and a dwell time of 5 s at each step. The initial kaolinite samples were powder mounted on aluminum frames. The altered mineral suspensions were quickly dried on glass slides under a heating lamp. Infrared (IR) spectra were recorded with a Perkin Elmer Spectrum GX FTIR System spectrometer. Samples KGa-1-STW1-8-weeks and KGa-1-STW3-8-weeks were pressed into KBr pellets (<1% w/w) and heated at 150ºC or 350ºC overnight before IR analysis. The IR instrument was purged with dry and low-$CO_2$ air produced by a Whatman Lab Gas Generator (Haverhill, MA). Electron micrographs were obtained with a Hitachi S-570 scanning electron microscope (SEM) operated at 25 kV. Powder samples were mounted directly on carbon conductive tabs, and sputter coated with gold before SEM analysis.

### *Stability of cancrinite and sodalite in acidic conditions*

A series of 0.05 g samples of KGa-1-STW3-8-weeks were mixed with 20 mL solutions containing different amounts of HCl in 40 mL Nalgene centrifuge tubes. The tubes were shaken overnight at room temperature and centrifuged. The supernatant solutions were collected for pH, $Na^+$ and $Al^{3+}$ analyses. The released $Na^+$ and $Al^{3+}$ were quantified with a Varian 220 Flame Atomic

Table 1. Chemical compositions of simulated tank waste (STW) solutions.

| Simulant solutions | NaOH (mol/kg) | $NaAlO_2$ (mol/kg) | $NaNO_3$ (mol/kg) |
|---|---|---|---|
| STW1 | 1.4 | 0.125 | 3.7 |
| STW2 | 2.8 | 0.125 | 3.7 |
| STW3 | 1.4 | 0.250 | 3.7 |
| STW4 | 2.8 | 0.250 | 3.7 |

https://doi.org/10.1346/CCMN.2004.0520101 Published online by Cambridge University Press

Absorption Spectrometer (Varian Ltd., Mulgrave, Australia) at 589 and 309 nm, respectively. The remaining solids were washed with distilled water and oven dried at 50ºC before weighing and XRD analysis.

*Cesium sorption isotherms*

Cesium sorption isotherms were determined using the batch equilibration method using samples of KGa-1 reacted with STW1 and STW3 at 80ºC. 120 mg of powder samples were weighed into 40 mL polycarbonate Nalgene centrifuge tubes. 25 mL of 0.01 or 0.1 M $NaNO_3$, or 0.005 or 0.05 M $Ca(NO_3)_2$ background solution were added to each tube. An appropriate amount of $CsNO_3$ stock solution, prepared in the corresponding matrix solution, was spiked into the tubes. The initial $Cs^+$ concentrations ranged from 0 to 0.4 mmol/L. The tubes were shaken on a reciprocal shaker at ambient condition (~22ºC) for 24 h. Initial trials showed that the amount of $Cs^+$ sorbed changed by <1% after 2 h of reaction. The tubes were centrifuged for 30 min at 12,060 g. An aliquot of the supernatant solution was sampled for Cs quantification with the atomic absorption spectrometer at a wavelength of 852.1 nm. To suppress ionization, both standards and samples were spiked with 2 M KCl solution to reach a final concentration of 1000 mg/L K in solution before analysis. The pH values of the supernatant solutions at the end of the sorption experiments were between 8.2 and 8.9. Sorption isotherms were constructed by plotting amounts sorbed, *i.e.* the difference between the quantity of $Cs^+$ added and the quantity in the final solution, *vs.* concentrations remaining in solution.

*Accessibility of internal sites in cancrinite/sodalite*

Sodalite and cancrinite are not considered as typical zeolite minerals because of the difficulty of molecular diffusion in their frameworks (Coombs *et al.*, 1997). To test if the internal sites in cancrinite and sodalite are accessible by inorganic ions, 0.05 g of sample KGa-1–STW3-8-weeks were mixed with 15 mL of 0.5 M $KNO_3$, $CsNO_3$ or 0.25 M $Ca(NO_3)_2$ solutions in a 40 mL Nalgene centrifuge tube. The tubes were kept in an oven at 80ºC for 24 h. During the day time of the 24 h storage, the tubes were shaken for 20 min every 2 h. At the end of the 24 h treatment, the tubes were centrifuged, and ~15 mL of supernatant solution from each tube were collected for $Na^+$ quantification with the atomic absorption spectrometer. An additional 15 mL of the corresponding $KNO_3$, $CsNO_3$ or $Ca(NO_3)_2$ solutions were added to the tubes. The tubes were stored, shaken and centrifuged as in the first washing. The washing process was repeated six times in total. After the sixth washing with the electrolyte solutions, the solids in the tubes were washed three times with deionized water; 15 mL of water were used in each washing. All these experiments were duplicated. The solids were mounted on glass slides for XRD analysis.

## RESULTS

*Mineralogical phase transformation in KGa-1 at 80ºC*

The major mineral in the KGa-1 sample is kaolinite as indicated by its characteristic X-ray diffraction peaks at 0.71 nm (001) and 0.356 nm (002) (Figure 1, bottom pattern). It also contains a minor amount of anatase ($TiO_2$) (101 diffraction at 0.351 nm) and mica. When KGa-1 reacted with the simulant solution STW1, the most distinct changes reflected on the XRD patterns are the reduction in intensity of the kaolinite peaks and the appearance of cancrinite and sodalite peaks. The intensity of the kaolinite peaks reduced progressively with time during the 8 weeks of monitoring period, with cancrinite and sodalite peaks enhanced accordingly (Figure 1). The kaolinite peaks are negligible after 8 weeks of reaction. Cancrinite and sodalite have several common peaks located at 0.632, 0.365, 0.259 and 0.211 nm on their XRD patterns, yet cancrinite can be identified by its characteristic diffraction peaks at 0.324 nm (121), 0.274 nm (400), 0.469 nm (101) and 0.415 nm (210). Sodalite has a unique peak at 0.284 nm (310) which can be used to differentiate it from other minerals. Other characteristic peaks of sodalite at 0.446 and 0.400 nm were too weak. The relative height of the 310 diffraction peak of sodalite at 0.284 nm to the nearby 400 peak of cancrinite at 0.274 nm appeared to be constant after 1–8 weeks of reaction, indicating that both sodalite and cancrinite were thermodynamically stable under the experimental conditions.

The 101 peak of anatase at 0.351 nm remained on all of the XRD patterns during the 8 week monitoring period, indicating its stability in the caustic simulant solutions. Weak mica peaks (1.0 nm) were present in the patterns of the samples reacted for 1 and 2 weeks.

*Morphology of KGa-1 and new minerals under SEM*

Kaolinite particles in KGa-1 showed platy structure with hexagonal outlines even though there were discontinuities observed on certain edges (Figure 2a). Some plates stack together forming a vermicular structure. All of these morphologies are typical of kaolinite. The new cancrinite/sodalite precipitates formed after contacting the simulant solutions showed very different morphology from kaolinite. The sizes of most of the individual new grains are a few tenths of a μm or even less (Figure 2b). Some of the grains developed along two dimensions forming platy structures with diameters of ~0.5 μm (Figure 2,c,d). The new type of plate does not have the abrupt edges or flat surfaces of the kaolinite plates. Moreover, one very common feature formed by the new plates is their intergrowth by which open spheres, lepispheres, formed (Figure 2c,d). Another type of morphology, thin flakes with larger diameters, were occasionally observed in the reacted samples (*e.g.* a flake at the upper left corner of Figure 2c). The flakes were very often curled and they are believed to be mica.

https://doi.org/10.1346/CCMN.2004.0520101 Published online by Cambridge University Press

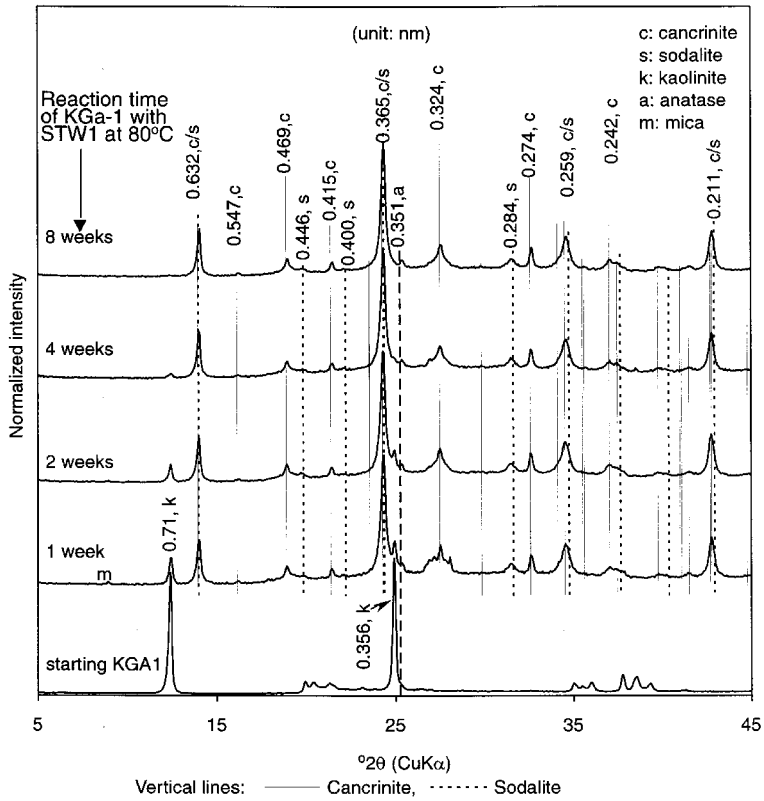


Figure 1. Normalized XRD patterns of KGa-1 kaolinite and the solid phases formed at different times following reaction with STW1 at 80°C. The vertical solid lines indicate the peak positions of cancrinite as published by Buhl *et al.* (2000). The vertical dotted lines indicate sodalite as published by Sieger *et al.* (1991). The dashed line is for anatase.

*Effect of aluminate concentration on mineral transformation rate*

When aluminate concentration was doubled to 0.25 M as in the simulant solution STW3, similar mineral phase transformations occurred in the kaolinite samples. The small lepispheric morphology as in Figure 2b,c was observed. The mineral transformation rate in STW3, however, appeared slower than that in STW1. More kaolinite remained in STW3 than in STW1 after the same reaction time (Figure 3). Kaolinite peaks are still visible on the XRD pattern of the sample reacted for 8 weeks with STW3. The slower transformation observed in STW3 compared to STW1 suggests that lower aluminate concentration in the simulant solution favors the dissolution of kaolinite and the formation of cancrinite and sodalite. Similar to the nearly constant cancrinite/sodalite ratio during the 8 weeks of reaction in STW1, the relative intensity of the 0.284 nm peak of sodalite to the 0.274 nm of cancrinite in STW3 did not show any obvious changes during the 8 weeks. Yet the 0.274, 0.324 and 0.469 nm peaks of cancrinite in the samples formed in STW3 are stronger than the corresponding peaks of cancrinite formed in STW1. This might be an indication of more cancrinite formed after reacting with STW3. We have also observed that the intensities of these peaks are strongly correlated to the crystallinity of cancrinite. The more crystalline cancrinite produced stronger diffraction peaks at these three positions (data not shown).

*Incorporation of nitrate in cancrinite/sodalite*

There were several distinct changes on the Fourier transform infrared (FTIR) spectra (Figure 4) when KGa-1 reacted with the simulated solutions. The characteristic OH-stretching vibrations of kaolinite at 3695, 3669, 3652 and 3620 $cm^{-1}$ disappeared or weakened after reacting with the simulated solutions. Other kaolinite bands at 938 $cm^{-1}$ (surface OH bending), and 914 $cm^{-1}$(inner OH bending) were also weakened. The reduction of the kaolinite bands in the solid phase formed in STW1 was more extensive than that in STW3. Weak kaolinite bands at 3695$cm^{-1}$ (surface OH) and 3620 $cm^{-1}$ were still visible in sample KGa-1-STW3-8-weeks. Coincident with the reduction or disappearance of kaolinite, cancrinite and sodalite bands appeared on the IR spectra, including the asymmetric Al–O stretch of cancrinite and sodalite located in the range 980–1120 $cm^{-1}$, and the symmetric Al–O stretch the minerals located in the range 660–770 $cm^{-1}$. The bands in the range 560–630 $cm^{-1}$ arose from the parallel 4- or 6-membered double rings of cancrinite and sodalite. The bands with wavenumbers <500 $cm^{-1}$ arose from the

https://doi.org/10.1346/CCMN.2004.0520101 Published online by Cambridge University Press

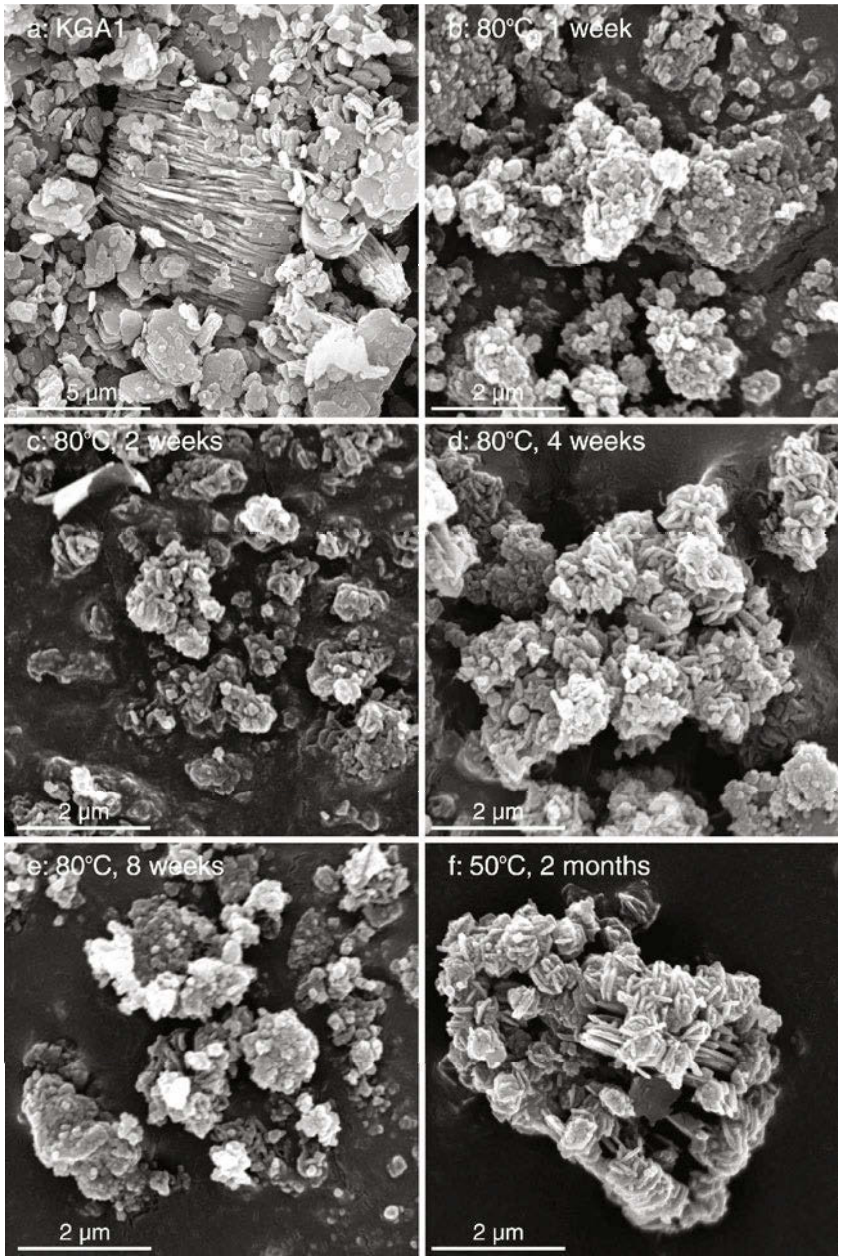


Figure 2. Mineral morphology change of KGa-1-kaolinite after reacting with STW1 for different times; (a) starting KGa-1 kaolinite with vermiform structure; (b–e) after 1, 2, 4, 8 weeks of reaction at 80ºC, respectively; (f) after 2 months of reaction at 50ºC.

bending vibrations of Si–O and Al–O of the tetrahedra of the feldspathoids. The detailed IR assignments for cancrinite and sodalite were summarized by Barnes *et al.* (1999b). Based on our pure mineral analyses (data not shown), the characteristic bands of cancrinite are located at 1113, 1032, 821, 618, 571 and 503 $cm^{-1}$. Sodalite can be distinguished by its bands at 733 and 707 $cm^{-1}$. The band positions shown in Figure 4 are slightly different from the bands observed in pure minerals, presumably due to crystallinity differences between the samples in this experiment and the synthetic pure minerals.

The FTIR spectra indicate that $NO_3^-$ was incorporated in the precipitates, the 1422 and 1384 $cm^{-1}$ bands being attributed to the $NO_3^-$ group. Our IR analysis of pure minerals showed that nitrate-cancrinite has only one $NO_3^-$ band at 1422 $cm^{-1}$. The 1384 $cm^{-1}$ band arose from either sodalite or $NaNO_3$ residue. Pure $NaNO_3$ salt alone has a band at 1384 $cm^{-1}$. It has been observed that pure nitrate-sodalite has a distinct $NO_3^-$ band at 1380 $cm^{-1}$ (Buhl and Loens, 1996). It is likely that the 1384 $cm^{-1}$ band belonged to the nitrate group in sodalite, because free $NaNO_3$ should have been removed

https://doi.org/10.1346/CCMN.2004.0520101 Published online by Cambridge University Press

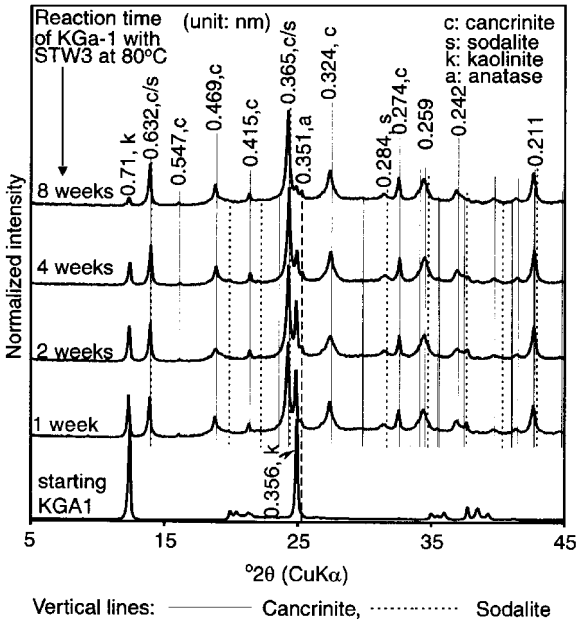


Figure 3. Normalized XRD patterns of KGa-1 kaolinite and the solid phases reacted for different times with STW3 at 80ºC.

after extensive dialysis against deionized water. When the samples were heated at 350ºC overnight, an additional band appeared at 1351 $cm^{-1}$ in both the KGa-1-STW1-8-weeks and KGa-1-STW3-8-weeks samples, and the 1422 $cm^{-1}$ band was weakened. It is likely that the 1351 $cm^{-1}$ band arose from the dehydrated nitrate group. The broad bands around 3500 $cm^{-1}$ indicate that water remained in the feldspathoids even after heating overnight at 150ºC. Heating the samples at 350ºC reduced the moisture content as reflected by the near disappearance of the broad band around 3500 $cm^{-1}$.

The FTIR spectra also indicate that NaOH was not incorporated to a significant extent in the cancrinite or sodalite lepispheres formed under the experimental conditions even though 1.4 M NaOH was used in the simulant solutions. There is no sharp NaOH band in the typical OH-stretching band range (3000–4000 $cm^{-1}$) after the samples were heated at 350ºC. In a highly crystalline sodalite formed in 16 M NaOH, we found a sharp band at 3640 $cm^{-1}$ that was attributed to the incorporated NaOH (data not shown). The lack of NaOH bands in cancrinite/sodalite lepispheres in this experiment indicate that cancrinite and sodalite prefer nitrate groups to hydroxide groups in their cages or channels under the conditions used.

*Mineral transformation at lower temperature (50ºC)*

When KGa-1 reacted with the simulant solutions at 50ºC, mineral transformation appeared to be similar to the transformation at 80ºC but with a slower reaction rate. Contrary to the near complete dissolution of kaolinite at 80ºC, kaolinite was still dominant after 2 months of reaction at 50ºC (Figure 5). The area of the 001 peak of kaolinite at 0.71 nm and the common 110 peaks of cancrinite and sodalite at 0.632 nm were used to estimate roughly the quantity of undissolved kaolinite based on the percentage of each peak area. Calculation indicated 65–75% of the solids was undissolved kaolinite. The total percentage of cancrinite and sodalite increased from 28% to 34% when NaOH concentration was raised from 1.4 to 2.8 mol/kg at 0.125 mol/kg $NaAlO_2$ level, and from 22% to 25% at 0.25 mol/kg

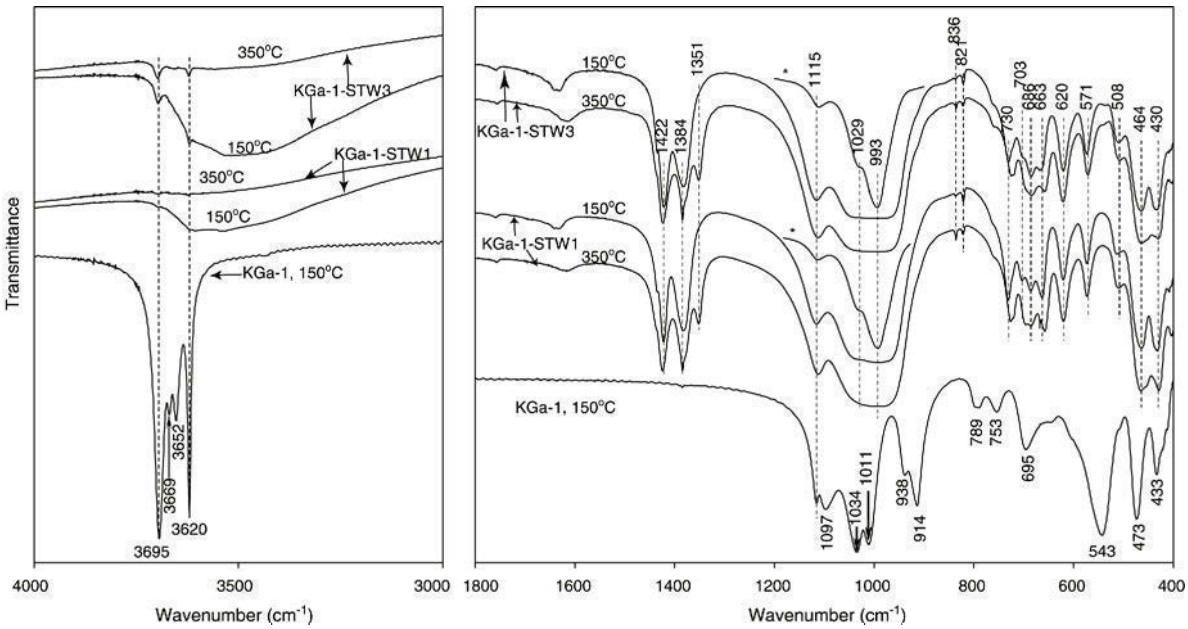


Figure 4. FTIR spectra of KGa-1 and samples KGa-1-STW1-8-weeks and KGa-1-STW3-8-weeks. The pellets were heated overnight at 150ºC and 350ºC, respectively. The asterisk-marked spectra were recorded with less concentrated unheated samples.

https://doi.org/10.1346/CCMN.2004.0520101 Published online by Cambridge University Press

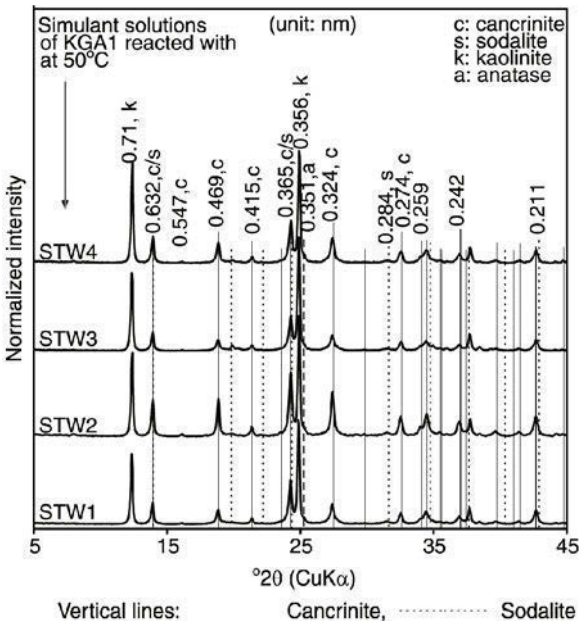


Figure 5. Normalized XRD patterns of KGa-1 reacted with four simulant solutions for 2 months at 50ºC.

$NaAlO_2$ level. These data also suggest that the cancrinite and sodalite yield was reduced when aluminate concentration was doubled at the same NaOH concentration level. Cancrinite and sodalite formed at 50ºC also showed the lepispheric structure (Figure 2f). Combining the information from Figures 1, 3 and 5, we conclude that increasing temperature, increasing NaOH concentration, and decreasing aluminate concentration facilitate the transformation of kaolinite to cancrinite and sodalite.

*Effect of kaolinite crystallinity on the transformation*

The mineral transformation of the poorly crystalline KGa-2 in the simulant solutions was similar to that of KGa-1. The XRD patterns of the resulting solids of KGa-2 after reacting with the simulant solutions were very similar to those in Figures 1, 3 and 5, and therefore are not shown here. No obvious morphology differences have been observed on the new mineral phases that formed from KGa-1 and KGa-2 kaolinites. The lack of a difference in the products formed from KGa-1 and KGa-2 kaolinites indicates that the reactant crystallinity is not an important factor in determining the mineral phases in alkaline solutions.

*Stability of cancrinite and sodalite under acidic conditions*

Cancrinite and sodalite were vulnerable to acid attack. When sample KGa-1-STW3-8-weeks was treated with HCl, the amount of $Na^+$ and $Al^{3+}$ released to the solution increased with increasing HCl concentration (Figure 6a). When the pH of the suspension was reduced to 5.5 by adding 0.24 mmol of HCl, 0.25 mmol of $Na^+$, nearly 90% of the total $Na^+$ in the sample, and 0.09 mmol of $Al^{3+}$ were released to the solution. The mass of solid was reduced by nearly 50%. The release of $Na^+$ and $Al^{3+}$ and the loss of the solid mass indicate pronounced dissolution of cancrinite and sodalite at pH 5.5. The released $Al^{3+}$ concentration did not increase in synchrony with that of $Na^+$. The lag of $Al^{3+}$ release to the solution indicates that there are other forms of Al-containing solids formed in weak acidic conditions. X-ray diffraction analysis indicates that only residual kaolinite, mica and anatase remained as the crystalline phases in the solid after treating with a large amount of acid (Figure 6b). Between pH 5.5 and 3.65, the diffraction patterns were noisy and broad humps occurred around 30º2θ, indicating poorly diffracting materials in the samples. When the pH was reduced from 3.65 to 1.4, the diffraction of residual kaolinite and mica enhanced progressively, indicating the loss of the amorphous phase. The XRD patterns also suggest that more anatase dissolved in the lower pH conditions as reflected by its reduced 101 diffraction at 0.351 nm relative to the kaolinite peak.

*$Cs^+$ adsorption*

Most Cs isotherm curves showed L-type adsorption on samples KGa-1-STW1 and KGa-1-STW3 (see Figures 7 and 8). The L-type isotherms were fitted with the Langmuir equation:

$$q = q_{max}\, KC/(1 + KC) \quad (1)$$

Where $q$ is the amount adsorbed, $q_{max}$ is the maximum adsorption capacity of the solid phase, K is the Langmuir constant, and $C$ is the final Cs aqueous concentration. The Langmuir parameters (Table 2) were determined by the normal nonlinear least-square method as recommended by Schulthess and Dey (1996). The newly formed cancrinite and sodalite showed much greater adsorption for Cs than kaolinite given the same Cs solution concentration. Generally, there was a 4–6 times increase in $Kq_{max}$ for Cs adsorption on the new minerals compared to KGa-1. Adsorption did not reach plateaux in the Cs solution concentration range tested. The ideal maximum adsorption should be equal to the CEC of each sample. Based on the formula $Na_6Al_6Si_6O_{24}{\cdot}2NaX$ of cancrinite and sodalite, the theoretical CEC of the fully dehydrated minerals should be in the range of 704–879 cmol/kg depending on the incorporated anion $X$, assuming that all of the $Na^+$ cations are exchangeable. The maximum adsorption capacities estimated from the sorption isotherms (Table 2) were far below the theoretical CEC of the feldspathoids; this is probably the result of the strong competition from the cations in the background solutions. The calculated maximum adsorption $q_{max}$ in 0.01 M $NaNO_3$ was nearly 9–12 times higher after reacting with the simulant solutions. The new solids formed in STW1 after 1, 2, 4 and 8 weeks displayed very

https://doi.org/10.1346/CCMN.2004.0520101 Published online by Cambridge University Press

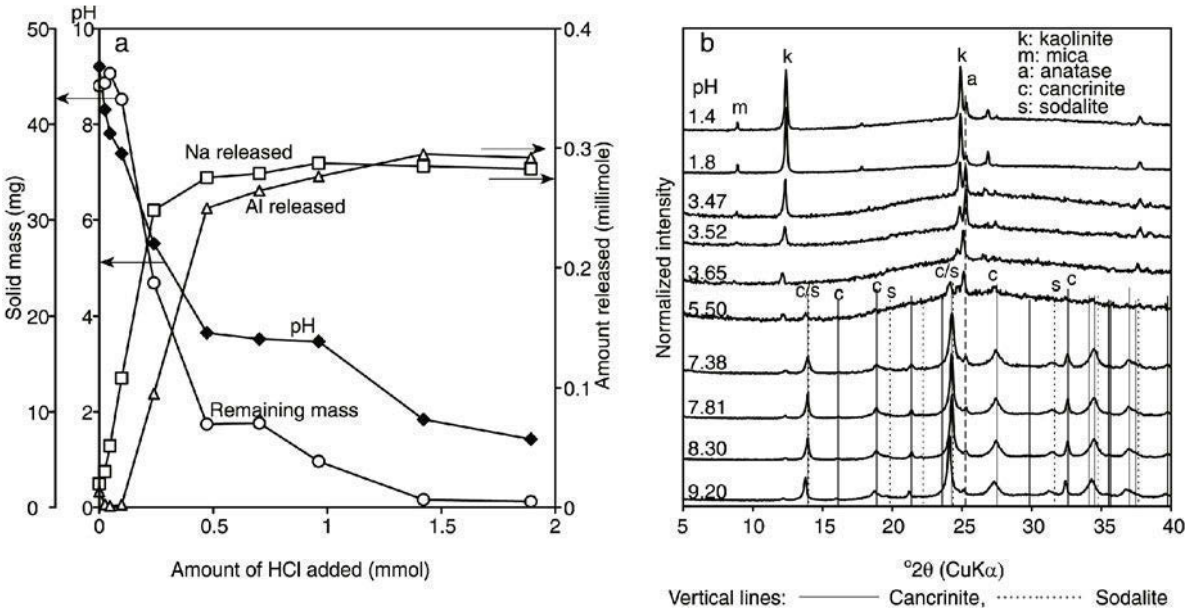


Figure 6. Acid attack on sample KGa-1-STW3-8-weeks, (a) remaining solid mass, released $Na^+$ and $Al^{3+}$, and suspension pH, and (b) XRD patterns of residue.

similar adsorption isotherms indicating that the mineral composition of the solid phase was fairly constant over the 8 week period. The precipitates formed in STW3 showed higher Cs adsorption than the corresponding precipitates formed in STW1, and the STW3 solids showed higher $Cs^+$ sorption with increasing reaction time (Figure 7). Since there is more kaolinite remaining after reacting with STW3, the difference observed on $Cs^+$ sorption is more likely to be caused by the relative amount of cancrinite to sodalite in the samples. It appears that cancrinite has a greater adsorption capacity than sodalite. The XRD peaks of cancrinite in KGa1-STW3-8-weeks were stronger than in KGA1-STW1-8-weeks as shown in Figures 1 and 3.

### *Cation competition in $Cs^+$ adsorption*

Cations in the background electrolyte solutions compete for sorption sites on cancrinite and sodalite. Samples KGa1-STW1-8-weeks and KGa1-STW3-8-weeks had very similar responses to the concentration change of the background electrolytes (Figure 8). When the background electrolyte concentration was increased, Cs adsorption decreased. Yet, the cations with different valence in the background electrolytes had different

Table 2. Langmuir parameters for $Cs^+$ sorption calculated with nonlinear regression analysis.

| Sample | Background electrolyte | $q_{max}$ (cmol/kg) | K (L/mmol) | Initial slope (L/kg) | Correlation coefficient† $n^{*2}$ |
|---|---|---|---|---|---|
| KGa-1-STW1, 1 week | 0.01 M $NaNO_3$ | 6.70 | 2.94 | 197.3 | 0.997 |
| KGa-1-STW1, 2 weeks | 0.01 M $NaNO_3$ | 5.31 | 4.53 | 241.1 | 0.997 |
| KGa-1-STW1, 4 weeks | 0.01 M $NaNO_3$ | 5.61 | 4.05 | 226.7 | 0.999 |
| KGa-1-STW1, 8 weeks | 0.01 M $NaNO_3$ | 4.65 | 6.23 | 289.8 | 0.999 |
| KGa-1-STW3, 1 week | 0.01 M $NaNO_3$ | 5.39 | 5.38 | 289.9 | 0.999 |
| KGa-1-STW3, 2 weeks | 0.01 M $NaNO_3$ | 5.83 | 5.22 | 304.6 | 0.999 |
| KGa-1-STW3, 4 weeks | 0.01 M $NaNO_3$ | 5.73 | 5.58 | 319.5 | 0.999 |
| KGa-1-STW3, 8 weeks | 0.01 M $NaNO_3$ | 6.14 | 6.40 | 393.1 | 0.999 |
| KGa-1-STW1, 8 weeks | 0.1 M $NaNO_3$ | 0.93 | 2.85 | 26.5 | 0.932 |
| KGa-1-STW3, 8 weeks | 0.1 M $NaNO_3$ | 5.79 | 0.59 | 34.3 | 0.995 |
| KGa-1-STW1, 8 weeks | 0.005 M $Ca(NO_3)_2$ | 4.12 | 2.83 | 116.8 | 0.990 |
| KGa-1-STW3, 8 weeks | 0.005 M $Ca(NO_3)_2$ | 6.54 | 2.65 | 173.4 | 0.996 |
| KGa-1-STW1, 8 weeks | 0.05 M $Ca(NO_3)_2$ | 2.04 | 3.46 | 70.6 | 0.988 |
| KGa-1-STW3, 8 weeks | 0.05 M $Ca(NO_3)_2$ | 4.41 | 2.33 | 102.7 | 0.996 |
| KGa-1 | 0.01 M $NaNO_3$ | 0.54 | 11.41 | 61.8 | 0.995 |
| KGa-1 | 0.1 M $NaNO_3$ | 0.92 | 1.01 | 9.3 | 0.948 |

† $n^{*2}$ assumes that a normal minimum correlates best (Schulthess and Dey, 1996)

https://doi.org/10.1346/CCMN.2004.0520101 Published online by Cambridge University Press

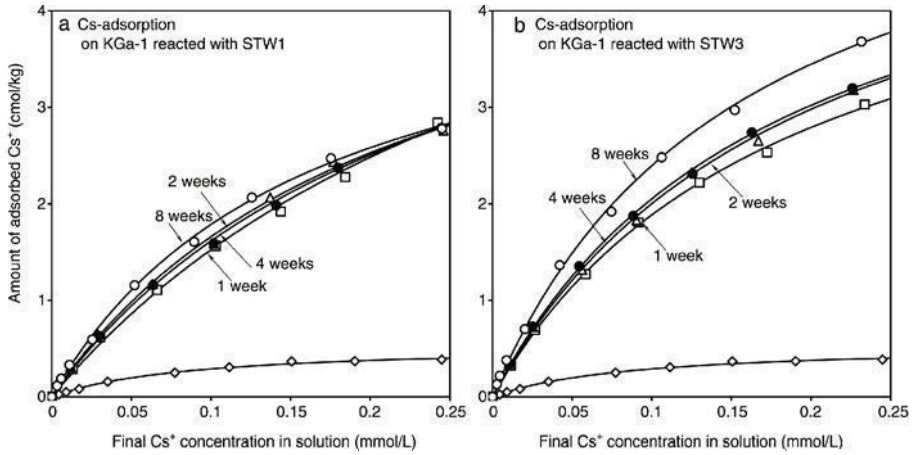


Figure 7. Cesium adsorption isotherms and fitted Langmuir curves of KGa-1 and the solid phases after reacting with (a) STW1 and (b) STW3 for 1, 2, 4 and 8 weeks at 80ºC. The background electrolyte was 0.01 M $NaNO_3$, and the pH of the final solutions was in the range 8.2–8.9.

competition capacities. At low ionic strength, *e.g.* 0.01 M $NaNO_3$ or 0.005 M $Ca(NO_3)_2$, the Cs adsorption in the 0.005 M $Ca(NO_3)_2$ was much lower than that in 0.01 M $NaNO_3$, indicating stronger competition from $Ca^{2+}$ than from $Na^+$. When the concentration of the two background electrolytes was increased by 10 times, the reduction in $NaNO_3$ solution was more extensive than that in $Ca(NO_3)_2$ solution. Indeed, Cs adsorption in 0.05 M $Ca(NO_3)_2$ solution was greater than that in 0.1 M $NaNO_3$ solution even though the $Ca^{2+}$ and $Na^+$ still had the same charge concentration. The lower adsorption of $Cs^+$ in the presence of a high concentration of $Na^+$ compared to the same charge concentration of $Ca^{2+}$ runs counter to what is expected for exchange between divalent and monovalent cations on phyllosilicate clay minerals and soils (McBride, 1994). The ability of 0.1 M $Na^+$ to compete more effectively with $Cs^+$ than the 0.05 M $Ca^{2+}$ suggests that there are some sites that are accessible to $Na^+$ and $Cs^+$ but not to $Ca^{2+}$.

*Accessibility of internal sites in cancrinite/sodalite*

When the KGa-1-STW3-8-weeks sample was washed with pure $CsNO_3$, $Ca(NO_3)_2$ or $KNO_3$ solutions containing 0.5 M $NO_3^-$, a large amount of $Na^+$ was released in the first 24 h washing at 80ºC (Figure 9), indicating that $Na^+$ in the cages of cancrinite and sodalite was exchangeable. Twice the amount of $Na^+$ was released by the first $KNO_3$ washing as by $CsNO_3$ or $Ca(NO_3)_2$, indicating that $K^+$ is the most efficient cation in the ion-exchange reaction. Substantial amounts of $Na^+$ are still released from the third through the sixth washings with $CsNO_3$. The different amounts of $Na^+$ released from the sequential washings indicate that $Na^+$ ions can readily migrate out of or into the cages and channels of cancrinite and sodalite. Other cations, such as $Cs^+$, $K^+$ and $Ca^{2+}$ can access the internal part of the minerals, yet they had different abilities to access those sites. Potassium ions can easily diffuse into the minerals, whereas $Cs^+$ ions take longer to reach the same sites,

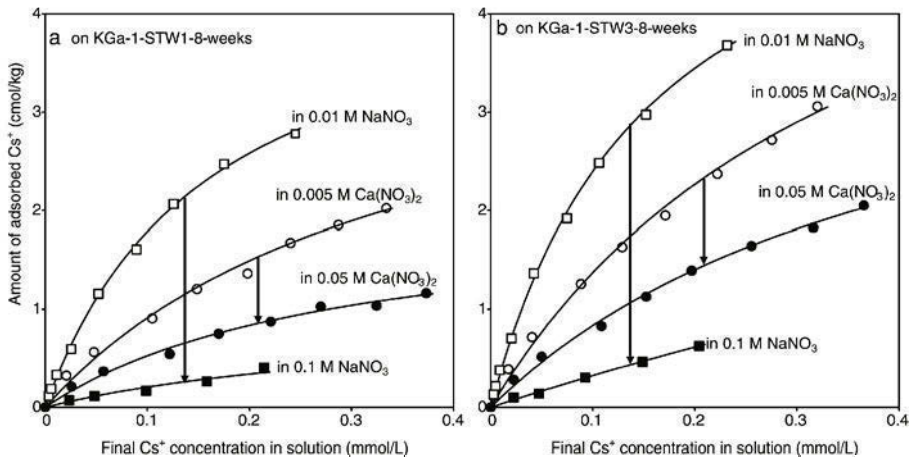


Figure 8. Cesium adsorption isotherms and fitted Langmuir curves of samples (a) KGa-1-STW1-8-weeks and (b) KGa-1-STW3-8-weeks. Background electrolytes are marked on the curves, and the pH of final solutions was in the range 8.2–8.9.

https://doi.org/10.1346/CCMN.2004.0520101 Published online by Cambridge University Press

presumably due to slower diffusion of the large $Cs^+$ ion. Calcium cations appeared to have the most difficulty in fully replacing the $Na^+$ even though the ionic radii of $Ca^{2+}$ and $Na^+$ are about the same (0.099 and 0.097 nm, respectively). That $Cs^+$ more easily accesses some sites occupied by $Na^+$ than does $Ca^{2+}$ explains the lower adsorption of $Cs^+$ in the 0.1 M $Na^+$ system relative to 0.05 M $Ca^{2+}$. $Na^+$ displaces $Cs^+$ on internal sites of cancrinite and sodalite which $Ca^{2+}$ cannot easily access.

The XRD patterns of the $CsNO_3$, $Ca(NO_3)_2$ and $KNO_3$ washed samples (Figure 10) indicate that $KNO_3$ washing expanded the minerals. For example, the common peak of cancrinite and sodalite at 0.632 nm was expanded to 0.656 nm, the 0.365 nm peak was expanded to 0.379 nm after $KNO_3$ washing. Similarly, the $d_{101}$ of cancrinite was expanded from 0.469 nm to 0.486 nm, the $d_{400}$ of 0.274 nm was expanded to 0.284 nm, the $d_{310}$ of sodalite was expanded from 0.284 nm to 0.293 nm. There was little, if any, expansion or shrinkage caused by Ca exchange. The $CsNO_3$ washing did not shift the diffraction peak positions, but weakened the diffraction at 0.632, 0.365 and 0.284 nm. The XRD diffraction intensity changes imply that the structure became more disordered when $Cs^+$ replaced the $Na^+$ in cancrinite and sodalite.

## DISCUSSION

### *Thermodynamic stability of cancrinite and sodalite*

The mineral phase transformation of kaolinite after contacting the simulated tank solutions indicates that there are two major processes involved in the reactions: dissolution of kaolinite releasing Si and Al (equation 2), and precipitation of the feldspathoids cancrinite and sodalite (equation 3).

$$Al_2Si_2O_5(OH)_4 + 6OH^- + H_2O = 2Al(OH)_4^- + 2H_2SiO_4^{2-} \quad (2)$$

$$6Al(OH)_4^- + 6H_2SiO_4^{2-} + 8\ Na^+ + 2X^- = Na_6Si_6Al_6O_{24}{\cdot}2NaX + 12OH^- + 12\ H_2O \quad (3)$$

where $X^-$ represents $NO_3^-$, $OH^-$ or $0.5CO_3^{2-}$.

Equation 2 suggests that the dissolution of kaolinite is favored at high NaOH concentrations, which is probably the reason why more kaolinite converted to cancrinite and sodalite in the 2.8 mol/kg NaOH solutions than in 1.4 mol/kg NaOH. Theoretically, kaolinite [$Al_2Si_2O_5(OH)_4$] dissolution releases Si and Al at a 1:1 ratio, and the formation of ideal cancrinite and sodalite also requires a 1:1 of Si to Al ratio. The presence of excess aluminate or silicate in the starting solution will drive the reaction to the left in equation 2. This is probably why doubling aluminate concentration in the simulant solutions resulted in more unaltered kaolinite. Equation 3 implies that high silicate and aluminate concentration will favor the formation of cancrinite or sodalite thermodynamically, and increased NaOH will inhibit the formation of the feldspathoids. The kaolinite to cancrinite and sodalite ratios reflected in Figures 1, 3 and 5 imply that the dissolution of kaolinite (equation 2) is the rate-determining step in the overall reaction.

The formation of cancrinite and sodalite has also been observed under similar experimental conditions. When synthetic Bayer liquors containing 3.9–5.4 M NaOH, 0.38 M $Na_2CO_3$, 1.6–2.33 M $Al(OH)_3$ and 0.1 M $SiO_2$ were heated to 250ºC in an autoclave, Linde type A zeolite, sodalite and cancrinite formed, and

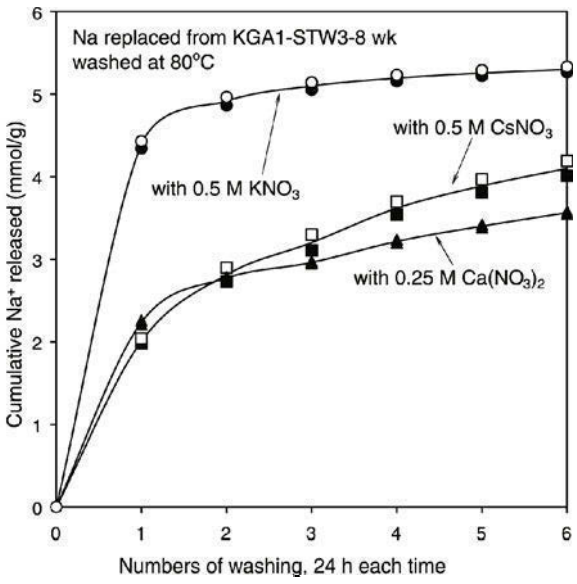


Figure 9. Released $Na^+$ from sample KGa-1-STW3-8-weeks. The sample was washed at 80ºC with 0.5 M $CsNO_3$, 0.25 M $Ca(NO_3)_2$ or 0.5 M $KNO_3$, respectively.

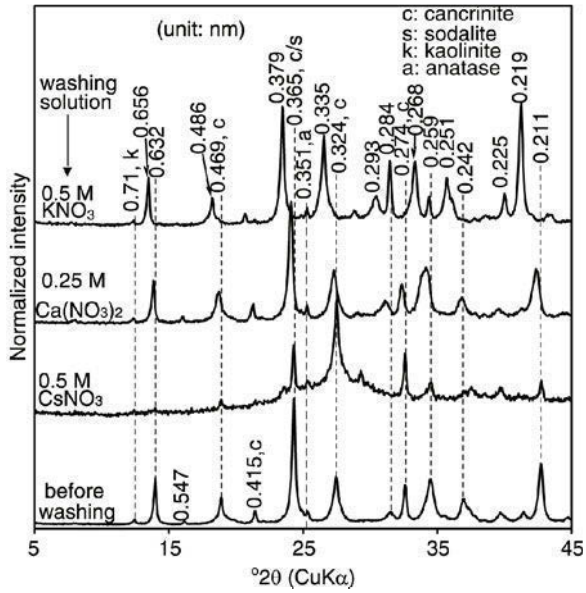


Figure 10. XRD patterns of sample KGa-1-STW3-8-weeks before and after six washings with $CsNO_3$, $Ca(NO_3)_2$ or $KNO_3$ solutions at 80ºC.

https://doi.org/10.1346/CCMN.2004.0520101 Published online by Cambridge University Press

cancrinite appeared more stable than sodalite (Barnes *et al.*, 1999a). It was proposed that the cancrinite would be the final product, whereas amorphous material, Linde type A zeolite and sodalite would be the transition phases (Barnes *et al.*, 1999a). The presence of a high concentration (*e.g.* 0.38 M) of sodium carbonate decreased the rate of cancrinite formation (Gerson and Zheng, 1997; Zheng *et al.*, 1997, 1998). Fetchtelkord *et al.* (2001) argued that sodalite is the thermodynamically more stable phase and cancrinite formation is kinetically favored at lower NaOH concentrations (<5 M) based on a series of tests in mixed solvents of butanediol and water. Combining these observations and our experimental results, it appears that the relative stability of sodalite and cancrinite depends on the initial chemical composition of the alkaline solutions. At high $NaNO_3$ concentration, such as the Hanford tank waste solutions, both cancrinite and sodalite are stable at NaOH concentration of 1.4 M. The consistent mineral phases observed at different temperatures, different NaOH or $NaAlO_2$ concentrations, and with different kaolinite sources are probably caused by the presence of high concentration of $NaNO_3$ in the experiment.

*Incorporation of ion pairs in cancrinite and sodalite*

The stoichiometry of cancrinite and sodalite has been reported as $Na_6Al_6Si_6O_{24}{\cdot}2NaX$, where $X$ is $1/2CO_3^{2-}$, $1/2SO_4^{2-}$, $Cl^-$, $OH^-$ or $NO_3^-$ (Barnes *et al.*, 1999a, 1999b). The crystal structure of cancrinite is similar to those of the zeolites, with a three-dimensional aluminosilicate host framework in which $Na^+$ and $Ca^{2+}$ cations, inorganic anions and water molecules exist as the guest components (Gerson and Zheng, 1997). The hexagonal cancrinite framework contains two main structural features: the ε-cages and the large 12-membered ring channel along the crystallographic *c* axis (Figure 11a), which can accommodate cations such as $Na^+$, $K^+$ and $Ca^{2+}$, as well as anions such as $CO_3^{2-}$, $OH^-$ and $NO_3^-$ (Barrer, 1978; Hund, 1984). The cubic sodalite structure can be described by the space-filling array of a $[4^66^8]$-truncated octahedron known as the sodalite- or β-cage (Figure 11b). Like cancrinite, each cage contains constituents of four water molecules or cation/anion pairs (Gerson and Zheng, 1997). The fundamental reason for the ability of cancrinite and sodalite to incorporate cation/anion pairs in their cages is their stability requirement. The Al/Si substitution in the sodalite framework requires three alkali metal cations within each β-cage to balance the charge of the $AlO_4^-$ unit on the framework. This requirement means that the three alkali cations will face each other directly in each cage and their repulsion makes the arrangement unstable. Incorporating a cation/anion ion pair inside the cage will compensate the direct cation-cation repulsion. The incorporated anion will be in the center of the β-cage, and a monovalent anion will tetrahedrally coordinate to the four alkali cations (Rabo, 1976). It has also been suggested that the ion pairs serve as a template during the formation of cancrinite and can stabilize the one-dimensional channel as a 'backbone' (Fechtelkord *et al.*, 2001).

Due to the high $NO_3^-$ concentration and high pH of the STWs, and the possibility of sorbing $CO_2$ from the atmosphere, the potential anions for the cancrinite/sodalite in our experiments are $NO_3^-$, $CO_3^{2-}$ and $OH^-$. Analysis by FTIR indicates that $NO_3^-$ is the major anion in the incorporated form. Carbonate or $OH^-$ did not incorporate to a detectable extent. Incorporated $CO_3^{2-}$ had two IR bands at 1410 and 1455 $cm^{-1}$ (Hackbarth *et al.*, 1999). The IR band of incorporated $CO_3^{2-}$ in sodalite synthesized in an autoclave has been reported at 1470 $cm^{-1}$(Barnes *et al.*, 1999c). No obvious bands near 1455 or 1470 $cm^{-1}$ on the FTIR spectra of the precipitates formed in our experiment. The two $NO_3^-$ bands at 1422 and 1384 $cm^{-1}$ which we observed suggested that both cancrinite and sodalite can incorporate $NO_3^-$ in the structure. Since $Na^+$ was the only cation in the system, the $NaNO_3$ ion pairs are expected to occur in the cages and channels of the feldspathoids.

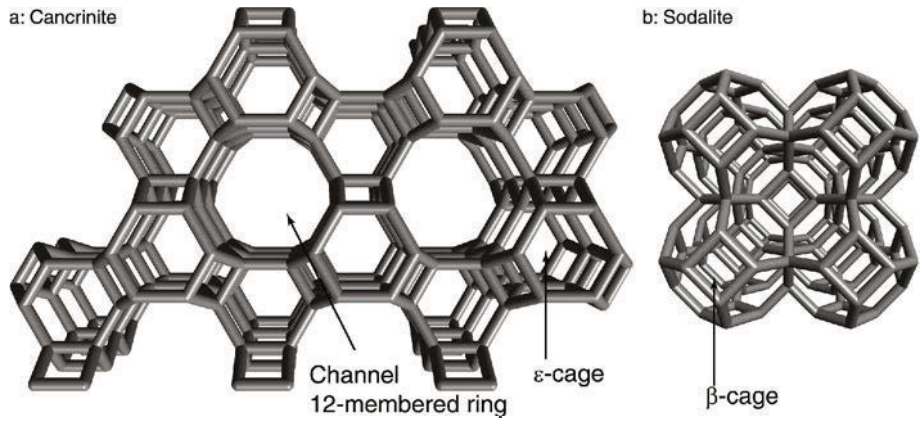


Figure 11. The 12-membered channel, ε-cage in cancrinite and the β-cage in sodalite frameworks. Images were generated with WebLab ViewerLite software (Accelrys, San Diego, California, USA) according to structural data published by the International Zeolite Association (www.iza-structure.org, accessed March 2003).

https://doi.org/10.1346/CCMN.2004.0520101 Published online by Cambridge University Press

*Accessibility of interior sites of cancrinite and sodalite*

The accessibility of cations to the interior of cancrinite and sodalite is dependent on the feldspathoid structure, and the size and valence of the cations. The 12-membered channel in cancrinite might be easier to access than the ε-cage. Access to the cages of cancrinite and sodalite requires that the cations be smaller than the aperture afforded by the 6-member rings. The free aperture size of hydrated sodalite is estimated as 0.22 nm (Breck, 1974), meaning that the cations must be dehydrated when they pass through the 6-member ring. The size limitation may explain why $Cs^+$ replaces $Na^+$ more slowly than does $K^+$. Divalent Ca has nearly the same ion radius as $Na^+$. It appears that $Ca^{2+}$ can migrate into the channels of the cancrinite, but not into the cages. One possible reason is the difficulty of $Ca^{2+}$ dehydration. The dehydration energy of $Ca^{2+}$ is 1650 kJ/mol, which is nearly three times as high as that of $Na^+$. Another possible reason is that it would be less favorable electrostatically to distribute two $Ca^{2+}$ cations as opposed to four $Na^+$ in the cages when the negative charges on the framework are strictly localized. It has been proposed that stacking faults in cancrinite could block channels and limit exchange and sorption (Bickmore *et al.*, 2001). The intergrowth of the plates observed in the cancrinite/sodalite lepispheres (Figure 2) implied that a joint interface of the two plates may cause a discontinuity in cancrinite channels; yet, 5.3 mmol/g or 530 cmol/kg of $Na^+$ released by $KNO_3$ washing (Figure 9) indicates that the internal $Na^+$ of sodalite and cancrinite are readily exchangeable.

## CONCLUSIONS

There were two major chemical processes involved in the reaction when kaolinite contacted the caustic simulant tank solutions: dissolution of kaolinite and formation of the feldspathoids cancrinite and sodalite. Kaolinite dissolution appeared to be the controlling step in the transformation. At the NaOH concentrations tested, cancrinite and sodalite particles have diameters of a few tenths of a μm or less. The new minerals form lepispheres by the intergrowth of their plates. Increasing NaOH concentration and temperature, and decreasing aluminate concentration in the initial solutions favor the dissolution of kaolinite and formation of cancrinite and sodalite. Both cancrinite and sodalite appeared stable under the experimental conditions, presumably because of the presence of a high concentration of $NaNO_3$ (3.7 M). Cancrinite and sodalite can incorporate $NaNO_3$ in their cages or channels. Little or no NaOH or $Na_2CO_3$ was incorporated under the experimental conditions. Cancrinite and sodalite are not stable under acidic conditions and pronounced dissolution occurred below pH 5.5. Cancrinite and sodalite have much higher Cs sorption capacities than kaolinite. This is because of the high degree of Al for Si substitution in the cancrinite and sodalite framework, whereas kaolinite has little or no Al for Si substitution. Cation exchange reactions indicate that $Na^+$ and $K^+$ can readily diffuse in cancrinite and sodalite, whereas Cs diffusion appeared relatively slow, presumably due to its large ionic radius. The frameworks of cancrinite and sodalite can be expanded by $K^+$ or become disordered by $Cs^+$. It is more difficult for $Ca^{2+}$ to access the internal sites of the minerals making $Ca^{2+}$ less competitive than $Na^+$ for $Cs^+$ sorption sites at high ionic strength.

## ACKNOWLEDGMENTS

This work was supported by the Environmental Management Science Program, US Department of Energy under contract DE-FG07-99ER62882. We thank the Electron Microscopy Center and the Department of Geology at Washington State University for the use of the SEM and FTIR equipment. Dr Daniel Strawn at the University of Idaho allowed us to use his FTIR spectrometer. We also thank three reviewers and the Associate Editor for their constructive comments.

## REFERENCES

Alberti, A., Colella, C., Oggiano, G., Pansini, M. and Vezzalini, G. (1994) Zeolite production from waste kaolin-containing materials. *Materials Engineering (Modena, Italy)*, **5**, 145–158.

Barnes, M.C., Addai-Mensah, J. and Gerson, A.R. (1999a) The mechanism of the sodalite-to-cancrinite phase transformation in synthetic spent Bayer liquor. *Microporous Mesoporous Materials*, **31**, 287–302.

Barnes, M.C., Addai-Mensah, J. and Gerson, A.R. (1999b) A methodology for quantifying sodalite and cancrinite phase mixtures and the kinetics of the sodalite to cancrinite phase transformation. *Microporous Mesoporous Materials*, **31**, 303–319.

Barnes, M.C., Addai-Mensah, J. and Gerson, A.R. (1999c) The solubility of sodalite and cancrinite in synthetic spent Bayer liquor. *Colloids and Surfaces A, Physicochemical and Engineering Aspects*, **157**, 106–116.

Barrer, R.M. (1978) *Zeolites and Clay Minerals as Sorbents and Molecular Sieves.* Academic Press, London, 496 pp.

Bauer, A., Velde, B. and Berger, G. (1998) Kaolinite transformation in high molar KOH solutions. *Applied Geochemistry*, **13**, 619–629.

Bickmore, B.R., Nagy, K.L., Young, J.S. and Drexler, J.W. (2001) Nitrate-cancrinite precipitation on quartz sand in simulated Hanford tank solutions. *Environmental Science and Technology*, **35**, 4481–4486.

Breck, D.W. (1974) *Zeolite Molecular Sieves: Structure, Chemistry, and Use.* John Wiley, New York, 752 pp.

Buhl, J.-c. (1991) Synthesis and characterization of the basic and non-basic members of the cancrinite-natrodavyne family. *Thermochimica Acta*, **178**, 19–31.

Buhl, J.-c. and Loens, J. (1996) Synthesis and crystal structure of nitrate enclathrated sodalite $Na_8[AlSiO_4]_6(NO_3)_2$. *Journal of Alloys and Compounds*, **235**, 41–47.

Buhl, J.-c., Stief, F., Fechtelkord, M., Gesing, T.M., Taphorn, U. and Taake, C. (2000) Synthesis, X-ray diffraction and MAS NMR characteristics of nitrate cancrinite $Na_{7.6}[AlSiO_4]_6(NO_3)_{1.6}(H_2O)_2$. *Journal of Alloys and Compounds*, **305**, 93–102.

Coombs, D.S., Alberti, A., Armbruster, T., Artioli, G., Colella, C. and Galli, E. *et al.* (1997) Recommended nomenclature

for zeolite minerals: report of the subcommittee on zeolites for the Internaltional Mineralogical Association, Commission on New Minerals and Mineral Names. *The Canadian Mineralogist*, **35**, 1571–1606.

Dudzik, Z. and Kowalak, S. (1974) Preparation of zeolites of faujasite type from kaolinite. *Przemyśl Chemiczny*, **53**, 616–618.

Fechtelkord, M., Posnatzki, B. and Buhl, J.-c. (2001) Synthesis of basic cancrinite in a butanediol-water system. *Chemistry of Materials*, **13**, 1967–1975.

Gephart, R.E. and Lundgren, R.E. (1998) *Hanford Tank Cleanup: A Guide to Understanding the Technical Issues.* 4th edition, Battelle Press, Columbus, Ohio.

Gerson, A.R. and Zheng, K. (1997) Bayer process plant scale: transformation of sodalite to cancrinite. *Journal of Crystal Growth*, **171**, 209–218.

Gualtieri, A., Norby, P., Artioli, G. and Hanson, J. (1997) Kinetic study of hydroxysodalite formation from natural kaolinites by time-resolved synchrotron powder diffraction. *Microporous Materials*, **9**, 189–201.

Hackbarth, K., Gesing, T.M., Fechtelkord, M., Stief, F. and Buhl, J.-c. (1999) Synthesis and crystal structure of carbonate cancrinite $Na_8[AlSiO_4]_6CO_3(H_2O)_{3.4}$, grown under low-temperature hydrothermal conditions. *Microporous Mesoporous Materials*, **30**, 347–358.

Hanlon, B.M. (1996) Waste tank summary report for month ending January 31, 1996 WHC-EP-0182-94. Westinghouse Hanford Company, Richland, WA.

Hund, F. (1984) Nitrate-, thiosulfate-, sulfate- and sulfide cancrinite. *Zeitschrift für Anorganische und Allgemeine Chemie*, **509**, 153–160.

McBride, M. (1994) *Environmental Chemistry of Soils*. Oxford University Press, New York, 406 pp.

Nyman, M., Krumhansl, J.L., Zhang, P., Anderson, H. and Nenoff, T.M. (2000) Chemical evolution of leaked high-level liquid wastes in Hanford soils. *Materials Research Society Symposium Proceedings*, **608**, 225–230.

Pruess, K., Yabusaki, S., Steefel, C. and Lichtner, P. (2002) Fluid flow, heat transfer, and solute transport at nuclear waste storage tanks in the Hanford vadose zone. *Vadose Zone Journal*, **1**, 68–88.

Rabo, J.A. (1976) Salt occlusion in zeolite crystals. Pp. 332–349 in: *Zeolite Chemistry and Catalysis* (J.A. Rabo, editor). ACS monograph **171**, American Chemical Society, Washington, D.C.

Schulthess, C.P. and Dey, D.K. (1996) Estimation of Langmuir constants using linear and nonlinear least squares regression analyses. *Soil Science Society of America Journal*, **60**, 433–442.

Serne, R.J., Zachara, J.M. and Burke, D.S. (1998) *Chemical information on tank supernatants, Cs adsorption from tank liquids onto Hanford sediments, and field observations of Cs migration from past tank leaks.* PNNL-11498/UC-510, Pacific Northwest National Laboratory, Richland, Washington.

Sieger, P., Wiebcke, M., Felsche, J. and Buhl, J.-c. (1991) Orientational disorder of the nitrite anion in the sodalite sodium aluminum silicate nitrite $(Na_8[AlSiO_4]_6(NO_2)_2)$. *Acta Crystallographica, Section C: Crystal Structure Communications*, **C47**, 498–501.

Zheng, K., Gerson, A.R., Addai-Mensah, J. and Smart, R.S.C. (1997) The influence of sodium carbonate on sodium aluminosilicate crystallization and solubility in sodium aluminate solutions. *Journal of Crystal Growth*, **171**, 197–208.

Zheng, K., Smart, R.S.C., Addai-Mensah, J. and Gerson, A. (1998) Solubility of sodium aluminosilicates in synthetic Bayer liquor. *Journal of Chemical and Engineering Data*, **43**, 312–317.

(*Received 26 April 2002; revised 27 August 2003; Ms. 651; A.E. James E. Amonette*)